PROCEEDINGS OF SCIENCE

Elastic and proton dissociative J/psi meson photoproduction at HERA

N. Gogitidze (on behalf of the H1 collaboration)
LPI, Moscow / DESY, Hamburg
E-mail: nellyg@mail.desy.de

Cross sections for elastic and proton-dissociative photoproduction of J/psi mesons are measured with the H1 detector in positron-proton collisions at HERA. The data were collected at ep centre-of-mass energies $\sqrt{s} \approx 318$ GeV and $\sqrt{s} \approx 225$ GeV, corresponding to integrated luminosities of $L = 130$ pb^{-1} and $L = 10.8$ pb^{-1}, respectively. The cross sections are measured as a function of the photon-proton centre-of-mass energy in the range $25 < W_{\gamma p} < 110$ GeV. Differential cross sections $\mathrm{d}\sigma/\mathrm{d}t$, where t is the squared four-momentum transfer at the proton vertex, are measured in the range $|t| < 1.2$ GeV^2 for the elastic process and $|t| < 8$ GeV^2 for proton dissociation. The results are compared to other measurements. The $W_{\gamma p}$ and t dependences are parametrised using phenomenological fits.

XXI International Workshop on Deep-Inelastic Scattering and Related Subjects - DIS2013,
22-26 April 2013, Marseille, France

1. Introduction

The results of the H1 collaboration on a measurement of diffractive J/ψ photoproduction in ep-interactions at HERA [1] are presented for the elastic scattering process, in which the outgoing proton stays intact and for the proton dissociative process, in which the proton dissociates into a low-mass hadronic system, as shown in figure 1 a) and b).

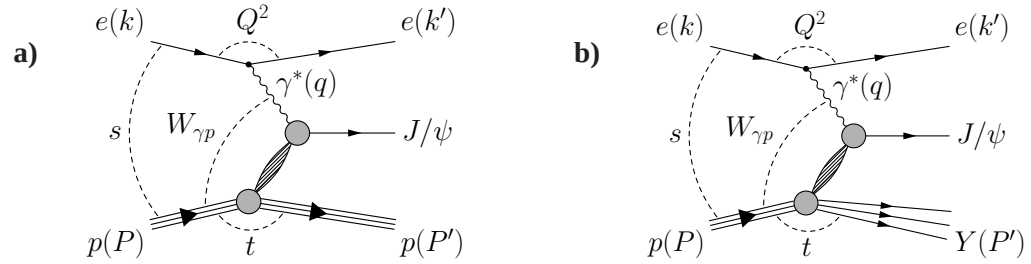

Figure 1: Diffractive J/ψ meson production in ep collisions: a) elastic and b) proton-dissociative.

Here s is the squared centre-of-mass energy of the ep system, $W_{\gamma p}$ the centre-of-mass energy of the virtual photon proton system, Q^2 the photon virtuality, i.e. the squared 4-momentum transfer at the electron vertex and t the squared 4-momentum transfer at the proton vertex. The results presented cover the range $25 \leq W_{\gamma p} \leq 110$ GeV, and the ranges $|t| < 1.2$ GeV^2 and $|t| < 8$ GeV^2 for the elastic and proton-dissociative processes, respectively.

Diffractive vector meson production is characterised by the t-channel exchange of a colourless object between the incoming photon and proton. In the high-energy limit Regge theory predicts energy dependent cross sections, $\sigma \propto W_{\gamma p}^{\delta}$ [2]. For light vector mesons (ρ, ω, ϕ) exponents $\delta \cong 0.22$ [3] are observed, compatible with a universal pomeron trajectory and an almost energy-independent cross-section. In contrast, the cross section for elastic J/ψ production rises more steeply with $W_{\gamma p}$, $\delta \cong 0.7$ [4, 5], and is thus incompatible with a universal pomeron.

In presence of a hard scale, here the mass of the J/ψ meson, perturbative calculations in QCD are possible. In pQCD the diffractive production of vector mesons can be described in the proton rest frame by a process in which the photon fluctuates into a $q\bar{q}$ pair at long distance from the proton target. The $q\bar{q}$ pair subsequently interacts with the proton via a colour-singlet exchange, which in lowest order QCD is a colourless gluon pair. The steep rise of the cross section with $W_{\gamma p}$ can be related to the rise of the square of the gluon density towards low values of Bjorken x. The $W_{\gamma p}$ dependence of proton-dissociative J/ψ production is expected to be similar.

Diffractive J/ψ production has been studied previously at HERA in the elastic regime at low values of $|t|$ [4, 5], and at very large values of $|t|$ [6, 7], where the dominant contribution is from proton-dissociative J/ψ production.

New in the presented results is the simultaneous determination of the cross sections in the elastic and proton dissociative regimes, without kinematic constraints on t. In addition to measurements at the nominal ep $\sqrt{s} \approx 318$ GeV, data taken at the lower energy $\sqrt{s} \approx 225$ GeV are also analysed. This low-energy data set provides new measurements in the transition region between high $W_{\gamma p}$ diffractive J/ψ measurements at HERA and the low $W_{\gamma p}$ fixed target experiments [8]. The elastic and proton-dissociative differential cross sections as a function of t and $W_{\gamma p}$ are analysed in fits, together with previous H1 data [4, 6].

2. Data Analysis

The measurement results are based on two data sets: 1) The data taken in the years 2006 - 2007, when HERA was operated with proton beam energy 920 GeV, resulting in $\sqrt{s} \approx 318$ GeV, corresponding to an integrated luminosity of 130 pb^{-1}; 2) The data recorded in 2007 before the final HERA shutdown, when the proton beam energy was reduced to 460 GeV, resulting in $\sqrt{s} \approx 225$ GeV, corresponding to an integrated luminosity of 10.8 pb^{-1}.

The H1 Fast Track Trigger (FTT) [9], which is based purely on charged track information, is used to trigger the events in both decay channels $J/\psi \to e^+e^-$, $\mu^+\mu^-$. The number of reconstructed J/ψ mesons is obtained from the invariant mass distributions m_{ll} in bins of t_{rec} and $W_{\gamma p,rec}$. These distributions for the muon and electron decay channels are shown in figure 2. In both distributions the J/ψ peak at $m_{ll} \sim 3.1$ GeV is clearly visible. In the electron channel the prominent tail of the mass peak towards lower mass values is due to QED radiation loss and bremsstrahlung from the electrons, reducing their momenta. There is also background from non-resonant QED processes $\gamma\gamma \to \mu^+\mu^-$ and $\gamma\gamma \to e^+e^-$, where one photon is radiated from the incoming positron and the other photon originates from the proton. Non-resonant diffraction contributes background to the $\gamma\gamma \to \mu^+\mu^-$ channel due to pions misidentified as muons. In contrast, the electron channel has negligible pion contamination near and above the J/ψ mass peak due to the superior background rejection in the electron selection.

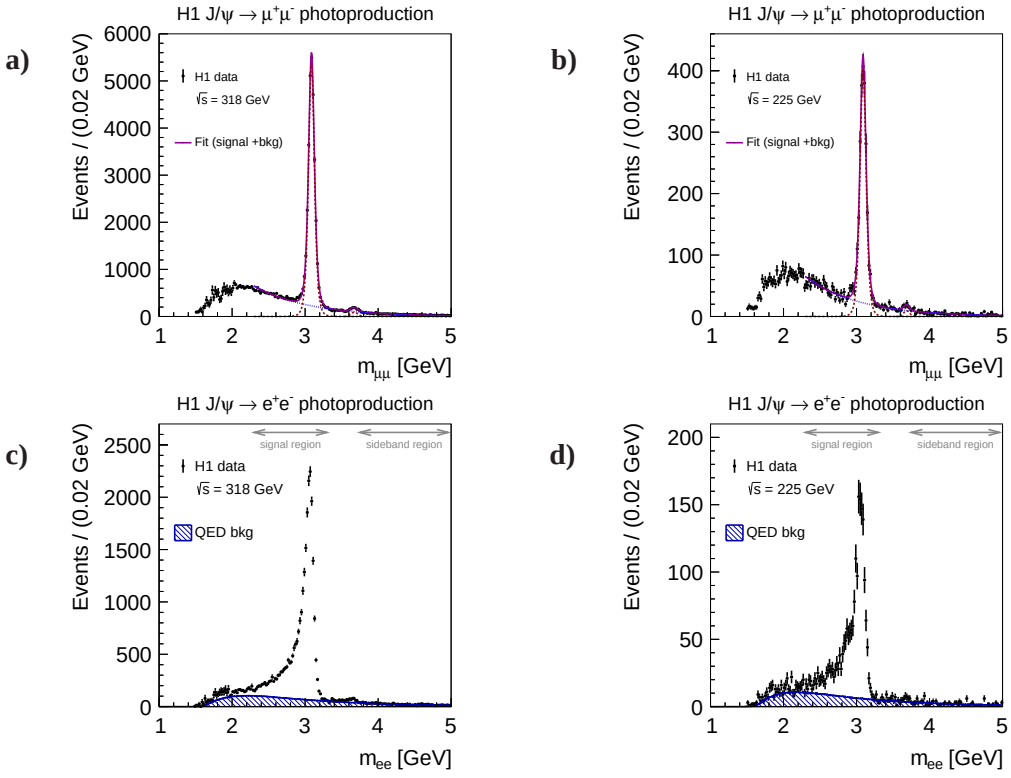

Figure 2: Di-lepton invariant mass distributions for the high- and low-energy data sets in the $J/\psi \to \mu^+\mu^-$ decay channel, figures a) and b) and in the $J/\psi \to e^+e^-$ decay channel, figures c) and d).

A tagging method is applied in both e^+e^- and $\mu^+\mu^-$ channels to disentangle the proton-dissociative candidates, either by requiring a large value of $t_{rec} \gtrsim 1.5$ GeV^2, or by requiring energy

deposition in the H1 forward detectors LAr, PLUG and Forward Tagging Stations (FTS).

3. Results

Regularised unfolding is used to determine the elastic and proton-dissociative cross section in bins of t and $W_{\gamma p}$ from the number of events observed as function of t_{rec} and $W_{\gamma p,rec}$, respectively, and from the forward tagging information. All details are discribed in [10].

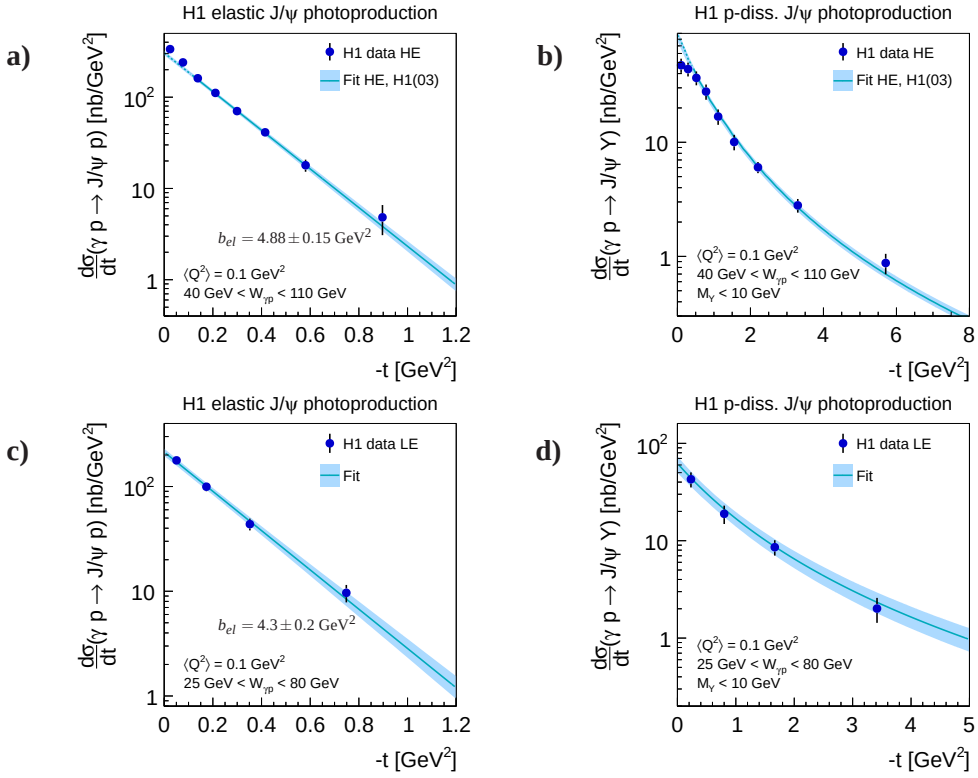

Figure 3: Differential J/ψ photoproduction cross section $d\sigma/dt$ as function of the negative squared four-momentum transfer at the proton vertex $-t$, as obtained in the high-energy data set a) and b), and in the low-energy data set c) and d), for elastic and proton-dissociative regime.

Figure 3 shows the measured elastic and proton-dissociative cross sections differential in $|t|$, separately for the high energy (HE) and low energy (LE) data sets. The cross sections fall steeply as a function of $|t|$, with a clear difference between the shapes of the proton-dissociative and elastic distributions. The proton-dissociative cross section levels off for very low values of $|t|$. There is a phase space effect such that for small $|t|$ it is not possible to produce large masses of M_Y.

The elastic and proton-dissociative differential cross sections $d\sigma/dt$ are fitted simultaneously, using a χ^2-function [11]. The elastic cross section is parametrised as $d\sigma/dt = N_{el}e^{-b_{el}|t|}$. For the proton-dissociative cross section the parametrisation $d\sigma/dt = N_{pd}(1+(b_{pd}/n)|t|)^{-n}$ is chosen, which interpolates between an exponential at low $|t|$ and a power law behaviour at high values of $|t|$. The fits are performed separately for HE and LE measurements. In the case of the HE data the previously measured high $|t|$ H1 data [6] are included in the fit. This fit yields a value

of $\chi^2/NDF = 26.6/18$ after excluding the two lowest $|t|$ data points in both the elastic and the proton-dissociative channel. For the fit of the LE data set, the parameter n is fixed to the value obtained from the HE data set, since the LE data are not precise enough to constrain b_{pd} and n simultaneously. The obtained parametrisations for the elastic and proton-dissociative cross sections are compared to the data in figure 3.

The elastic cross section data for $|t| > 0.1$ GeV are well described by the exponential parametrisation. Even at small $|t|$ they fall much faster with increasing $|t|$ than the proton-dissociative cross section, which is reflected in the values for b_{el} and b_{pd}. The extracted b_{el} value is compatible with previous results [4], although the previous fit was done as a function of $p^2_{T,J/\psi}$ rather than $|t|$. Some difference between the $b_{el,HE} = (4.88 \pm 0.15)$ GeV^2 and $b_{el,LE} = (4.3 \pm 0.2)$ GeV^2 values is expected due to the different $W_{\gamma p}$ ranges, $\langle W_{\gamma p} \rangle = 78$ GeV and $\langle W_{\gamma p} \rangle = 55$ GeV for the HE and LE data sets, respectively.

The measured elastic and proton-dissociative cross sections as a function of $W_{\gamma p}$ are shown in figure 4 a) and b). The elastic and proton-dissociative cross sections are of similar size at the lowest $W_{\gamma p} = 30$ GeV accessed in this analysis. The elastic cross section rises faster with increasing $W_{\gamma p}$ than the proton-dissociative one. The ratio of the proton-dissociative to the elastic cross section as a function of $W_{\gamma p}$, shown in figure 4 c), decreases from 1 to 0.8 as $W_{\gamma p}$ increases from 30 GeV to 100 GeV.

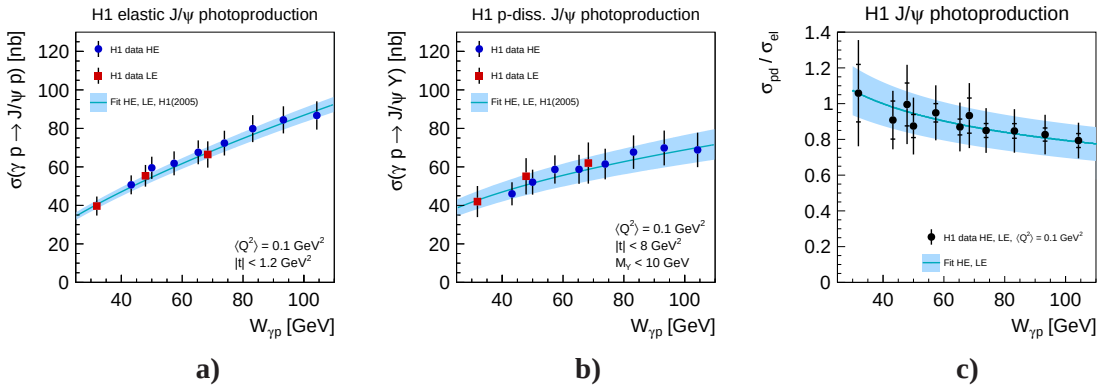

Figure 4: J/ψ photoproduction cross section as function of photon proton centre-of-mass energy $W_{\gamma p}$ for the a) elastic and b) proton-dissociative regime. c) is the ratio of the elastic to the proton-dissociative J/ψ photoproduction cross section as function of $W_{\gamma p}$.

The elastic and the proton-dissociative cross sections as a function of $W_{\gamma p}$ are fitted simultaneously, taking into account the correlations between these cross sections. The fit also includes data from a previous measurement [4] shown in figure 4, with a normalisation uncertainty of 5% and all other systematic uncertainties treated as uncorrelated. As parametrisation a power law function of the form $\sigma = N(W_{\gamma p}/W_{\gamma p,0})^{\delta}$ with $W_{\gamma p,0} = 90$ GeV is used, with separate sets of parameters for the elastic and the proton-dissociative cases.

The result of the fit is compared to the measurements in figure 4 a) and b). In Regge phenomenology the parameter δ can be related to the pomeron trajectory $\alpha(t) = \alpha(0) + \alpha' \cdot t$ by $\delta(t) = 4(\alpha(t) - 1)$. Using the values $\alpha'_{el} = 0.164 \pm 0.028 \pm 0.030$ Gev^{-2} [4] and $\alpha'_{pd} = -0.0135 \pm 0.0074 \pm 0.0051$ Gev^{-2} [6], together with the mean values of t for the elastic and proton-dissociative measurements, $\langle t \rangle = -0.2$ GeV^2 and $\langle t \rangle = -1.1$ GeV^2, one can estimate $\alpha(0)$ for the elastic and

proton-dissociative processes from these measured parameters. The obtained values of $\alpha(0)_{el} = 1.20 \pm 0.01$ and $\alpha(0)_{pd} = 1.09 \pm 0.02$ are in agreement with previous results.

The ratio of the two cross sections, shown in figure 4 c), gives a direct comparison between δ_{el} and δ_{pd}. The ratio is parametrised as $N_R(W_{\gamma p}/W_{\gamma p,0})^{\delta_R}$ with $W_{\gamma p,0} = 90$ GeV, $N_R = N_{pd}/N_{el} = 0.81 \pm 0.10$ and $\delta_R = \delta_{pd} - \delta_{el} = -0.25 \pm 0.06$, taking all correlations into account.

A compilation of cross section measurements for the elastic J/ψ photoproduction cross section is shown in figure 5 as a function of $W_{\gamma p}$.

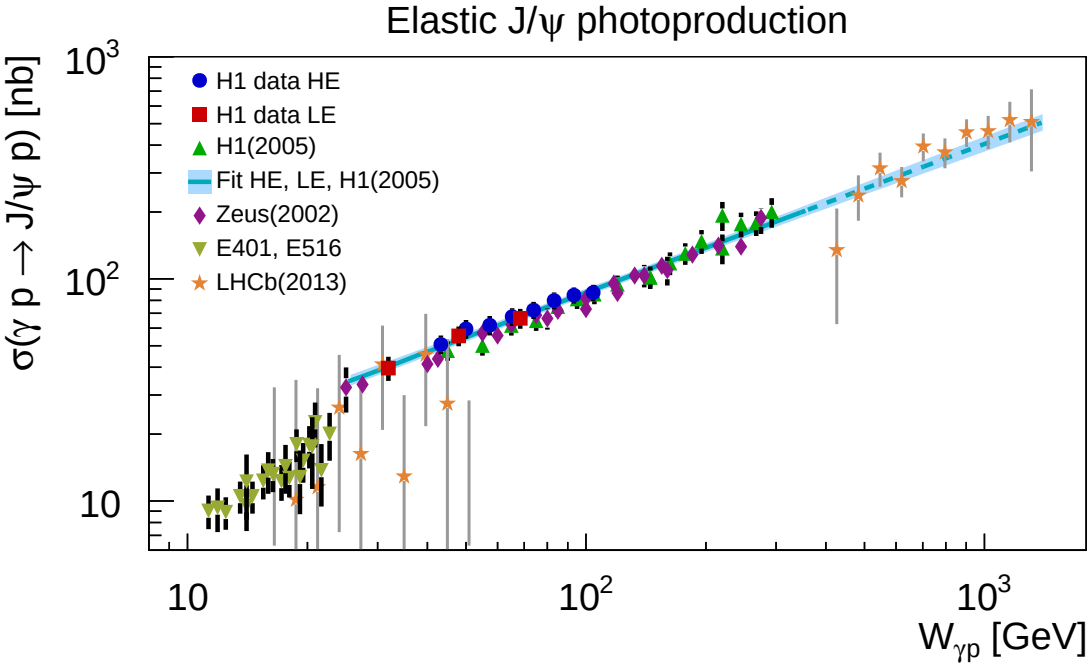

Figure 5: Compilation of various elastic J/ψ photoproduction cross section measurements including this measurement, previous HERA results [4, 5], results from fixed target experiments [8] and from LHCb [12]. The fit to the H1 data only is indicated by the curve. The fit has been extrapolated to higher values of $W_{\gamma p}$ (dashed curve). The spread of the surrounding band indicates the uncertainty of the fit.

The LE data from the present analysis fall in the gap between the data of fixed target experiments [8] at low $W_{\gamma p}$ and the bulk of the previous high $W_{\gamma p}$ HERA data. The fixed target data exhibit a lower normalisation and a steeper slope than observed at HERA. Also shown are recent results from the LHCb experiment [12]. The extrapolated fit function for the H1 elastic J/ψ photoproduction cross section describes the LHCb data points at high $W_{\gamma p}$ well.

4. Conclusions

Photoproduction cross sections for elastic and proton-dissociative diffractive J/ψ meson production have been measured as a function of T and $W_{\gamma p}$ in the kinematic ranges $|t| < 8$ GeV^2, 25 GeV $< W_{\gamma p} <$ 110 GeV and for the proton-dissociative case $M_Y < 10$ GeV. The data were collected in ep collisions with the H1 detector at HERA, at ep centre-of-mass energies $\sqrt{s} \approx 318$ GeV and $\sqrt{s} \approx 225$ GeV. Measurements in the electron and muon decay channels are combined and parametrised using phenomenological fits.

The elastic and the proton-dissociative cross sections are extracted simultaneously. A precise measurement of proton-dissociative J/ψ production is performed in the range of small $|t|$ for the first time. The data taken at low $W_{\gamma p}$ centre-of-mass energies fall in the gap between previous H1 measurements and fixed target data.

Acknowledgments

It is a pleasure to thank all my colleagues in H1, especially F. Huber and M. Sauter, for providing the data shown in this report and for their help given to me. I would also like to thank the organizers for creating a pleasant and inspiring conference atmosphere.

References

[1] C. Alexa et al. [H1 Collaboration], *Eur. Phys. J.* **C73** (2013) 2466 [arXiv:1304.5162].

[2] P. D. B. Collins, "An Introduction to Regge Theory and High Energy Physics", *Cambridge University Press*, 1977.
A. Donnachie and P. V. Landshoff, *Phys. Lett.* B **348** (1995) 213 [hep-ph/9411368].

[3] A. Levy, "Low x physics at HERA", *Lecture Notes in Physics*, **496**, (1997) 347-477, DESY-97-013, TAUP-2398-96.

[4] A. Aktas et al. [H1 Collaboration], *Eur. Phys. J.* **C46** (2006) 585 [hep-ex/0510016].

[5] S. Chekanov et al. [ZEUS Collaboration], *Eur. Phys. J.* **C24** (2002) 345 [hep-ex/0201043].

[6] A. Aktas et al. [H1 Collaboration], *Phys. Lett. B* **568** (2003) 205 [hep-ex/0306013].

[7] S. Chekanov et al. [ZEUS Collaboration], *JHEP* **1005** (2010) 085 [arXiv:0910.1235].

[8] M. E. Binkley et al. *Phys. Rev. Lett.* **48** (1982) 73.
B. H. Denby et al. *Phys. Rev. Lett.* **52** (1984) 795.

[9] A. Baird et al. *IEEE Trans. Nucl. Sci.* **48** (2001) 1276 [hep-ex/0104010];
D. Meer et al. *IEEE Trans. Nucl. Sci.* **49** (2002) 357;
N. Berger et al. *IEEE Nuclear Science Symposium Conference Record, volume 3,* (2004) 1976.

[10] F. Huber, "Elastic and proton-dissociative J/ψ Photoproduction at low $W_{\gamma p}$ with the H1 Detector at HERA", Ph.D. thesis, Heidelberg Univ. (2012), DESY-THESIS-2013-004 (at http://www-h1.desy.de/psfiles/thesis/).

[11] F. D. Aaron et al. [H1 Collaboration], *Eur. Phys. J.* **C63** (2009) 625 [arXiv:0904.0929].
F. D. Aaron et al. [H1 and ZEUS Collaborations], *JHEP* **1001** (2010) 109 [arXiv:0911.0884].

[12] R. Aaij et al. [LHCb Collaboration], *J. Phys.* G **40** (2013) 045001 [arXiv:1301.7084].